crystals

MDPI

Article

# Extended Assemblies of Ru(bpy)$(CO)_2X_2$ (X = Cl, Br, I) Molecules Linked by 1,4-Diiodotetrafluoro-Benzene (DITFB) Halogen Bond Donors

**Xin Ding, Matti Tuikka, Kari Rissanen and Matti Haukka ***

Department of Chemistry, University of Jyväskylä, P.O. Box 35, FI-40014 Jyväskylä, Finland; xin.dingharas@gmail.com (X.D.); MTU@dinex.fi (M.T.); kari.t.rissanen@jyu.fi (K.R.)

* Correspondence: matti.o.haukka@jyu.fi; Tel.: +358-40-8054666

Received: 20 May 2019; Accepted: 19 June 2019; Published: 24 June 2019


**Abstract:** The ruthenium carbonyl compounds, Ru(bpy)$(CO)_2X_2$ (X = Cl, Br or I) act as neutral halogen bond (XB) acceptors when co-crystallized with 1,4-diiodotetrafluoro-benzene (DITFB). The halogen bonding strength of the Ru-X···I halogen bonds follow the nucleophilic character of the halido ligand. The strongest halogen bond occurs between the chlorido ligand and the iodide atoms of the DITFB. All three halogen bonded complexes form polymeric assemblies in the solid state. In Ru(bpy)$(CO)_2Cl_2$·DITFB (1) and in Ru(bpy)$(CO)_2Br_2$·DITFB (2) both halido ligands are halogen bonded to only one DITFB donor. In Ru(bpy)$(CO)_2I_2$·DITFB (3) only one of the halido ligands is involved in halogen bonding acting as ditopic center for two DITFB donors. The polymeric structures of 1 and 2 are isomorphic wave-like single chain systems, while the iodine complexes form pairs of linear chains attached together with weak F···O≡C interactions between the closest neighbors. The stronger polarization of the iodide ligand compared to the Cl or Br ligands favors nearly linear C-I···I angles between the XB donor and the metal complex supporting the linear arrangement of the halogen bonded chain.

**Keywords:** halogen bond; ruthenium; crystal structure; bipyridine; carbonyl

## 1. Introduction

Halogen bond (XB) has found to be a useful tool in crystal engineering in recent years due to its strength and directional preferences [1–6]. A molecular entity with electrophilic region on a halogen atom is defined as XB donor, while an entity with nucleophilic region, i.e., Lewis base, is defined as an XB acceptor [7]. The strength and the directionality of halogen bond are well explained by σ-hole theory and by the nature of the elements attached to the halogen atoms [8–20]. Typical XB acceptors include covalently bonded nitrogen or sulfur atoms but also electron donors such as oxygen, selenium, and silicon are known to act as XB acceptors [21–24]. Even metal centers in square planar and linear metal compounds have shown XB acceptor properties [25–27]. Metal coordinated electron donor ligands provide another group of potential XB acceptors [28–36]. Especially metal halides are quite commonly used as XB acceptors. Even if coordination to a metal center is not usually enough to generate strong σ-hole on a halido ligand, the electron density around a coordinated halogen atom, X, is polarized [28,31]. This means that the M-X···X angle in a halogen bonded M-X···X-R system is typically ranging between 90° and 150°, depending on the nature of the metal center [13,30,31]. By using bidentate halogen bond donors, such as $I_2$, it is possible to link metal complexes together to form non-covalent metallopolymers [14,30,31,37–47]. However, $I_2$ is not necessarily the most desirable linking unit due to its redox behavior and its impact on the metal complex [45,47]. When the interaction between the metal coordinated halogen atom and the $I_2$ donor remains mainly electrostatic,

symmetrical bridges between the metal centers can be obtained. However, when the charge transfer and electron sharing, i.e., covalency, between the halogen atoms are increased, the electron distribution in the linking $I_2$ may change. This, in turn, may hamper the formation of symmetrical bridges and nature of the contacts between the linking unit and the metal complexes [31]. From this point of view, other XB donors, such as fluorinated iodobenzenes, behave more predictably as linkers in XB complexes and are, therefore, more reliable bridging units. In general, the motivation in building halogen bonded extended metal complex systems arises from the possibilities to modify the redox, magnetic, photophysical and optical properties of the complexes extended by halogen bonds [4,6,29,48].

Previously, we studied crystal structures and the nature of XBs in $I_2$ linked assemblies of $[Ru(bpy)(CO)_2X_2]$ (X = Cl, Br, I) compounds (Figure 1) [31]. Since the $I_2$ linkers XB properties are dependent on the nature of the halogen bond contacts, here, we used another potentially bridging XB donor, i.e., tetrafluorodiiodobenzene (DITFB, Figure 1) as the linker for $[Ru(bpy)(CO)_2X_2]$ molecules (X = Cl, Br, I). The goal was to further investigate the extended assemblies that can be obtained through XB by using organometallic $[Ru(bpy)(CO)_2X_2]$ molecules as XB acceptors.

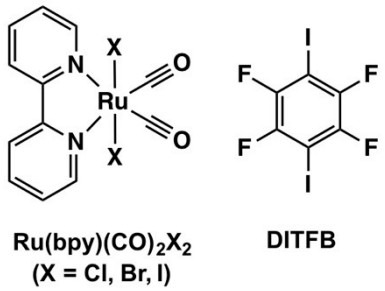


**Figure 1.** The schematic structures of $Ru(bpy)(CO)_2X_2$ (X = Cl, Br, I) and 1,4-diiodotetrafluorobenzene (DITFB).

## 2. Materials and Methods

### *2.1. Materials*

All reagents and solvents were obtained from commercial sources and were used as received. The syntheses and crystal structures of the parent metal compounds $[Ru(bpy)(CO)_2X_2]$ (X = Cl, Br, I) have been reported in the literature [49,50]. All co-crystallizations were optimized only for obtaining high-quality single crystals, not for obtaining maximum yields.

### *2.2. Syntheses of co-crystals 1–3*

**$[Ru(bpy)(CO)_2Cl_2]$·DITFB (1).** The light-yellow crystals were obtained by dissolving 5 mg of the metal complex and 10.5 mg of DITFB in $CH_2Cl_2$ solvent. The crystallization was carried out at room temperature by slow evaporation of the solvent. The X-ray quality crystals were harvested in two days.

**$[Ru(bpy)(CO)_2Br_2]$·DITFB (2).** The yellowish green crystals were obtained by dissolving 5 mg of the metal complex and 8.5 mg of DITFB in $CH_2Cl_2$ solvent. The crystallization was carried out at room temperature by slow evaporation of the solvent. The X-ray quality crystals were harvested in a week.

**$[Ru(bpy)(CO)_2I_2]$·DITFB (3).** The bright orange crystals were obtained by dissolving 5 mg of the metal complex and 7.1 mg of DITFB in $CH_2Cl_2$ solvent. The crystallization was carried out at room temperature by slow evaporation of the solvent. The X-ray quality crystals were harvested in a week.

### *2.3. X-ray Structure Determination*

The crystals of 1–3 were measured at 120 K on a Rigaku Oxford Diffraction Supernova diffractometer (Oxford Diffraction, Woodlands, Tex, USA) (1), or on a Bruker Kappa Apex II diffractometer (Bruker Nonius, Delft, The Netherlands) (2,3) using Mo Kα (λ = 0.71073 Å) radiation. The CrysAlisPro [51] or Apex2 [52] program packages were used for cell refinements and data reductions. Multi-scan

absorption corrections based on equivalent reflections (CrysAlisPro, Apex2, Yarnton, Oxfordshire, England) were applied to the intensities before structure solutions. The structures were solved by the charge flipping method using the SUPERFLIP [53] software or by the intrinsic phasing method using SHELXT (v. 2014/5) [54]. All structures were refined by using SHELXL program [54]. Both structures 1 and 2 contained voids with heavily disordered and partially lost solvent of crystallization. A series of crystals were analyzed, and the residual electron density was found to vary from crystal to crystal indicating a variable amount of solvent in different crystals. Therefore, the final structural models of 1 and 2 were refined without the solvent molecules, and the contribution of the missing solvent to the calculated structure factors were taken into account by using the SQUEEZE routine of PLATON(v. 141217) [55]. Since the amount of solvent could not be determined accurately, the missing solvent molecules were not taken into account in the unit cell content. The hydrogen atoms were positioned geometrically and constrained to ride on their parent atoms, with C-H = 0.95 Å and $U_{iso}$ = 1.2·$U_{eq}$ (parent atom). The crystallographic details are summarized in Table 1.

CCDC 1820788–1820790 contain the crystallographic data for 1–3, respectively. These data can be obtained free of charge via http://www.ccdc.cam.ac.uk/cgi-bin/catreq.cgi, or from the Cambridge Crystallographic Data Centre, 12 Union Road, Cambridge CB2 1EZ, UK; fax: (+44) 1223 336 033; or e-mail: deposit@ccdc.cam.ac.uk.

**Table 1.** Crystal Data.

| | **1** | **2** | **3** |
|---|---|---|---|
| Formulas | $C_{18}H_8Cl_2F_4I_2N_2O_2Ru$ [+ solvent] [+ solvent] | $C_{18}H_8Br_2F_4I_2N_2O_2Ru$ [+ solvent] | $C_{18}H_8F_4I_4N_2O_2Ru$ |
| Fw | 786.03 * | 874.95 * | 968.93 |
| temp (K) | 120(2) | 120(2) | 120(2) |
| $\lambda$(Å) | 0.71073 | 0.71073 | 0.71073 |
| Crystal system | Monoclinic | Monoclinic | Orthorhombic |
| space group | C2/c | C2/c | Pnma |
| *a* (Å) | 11.9736(7) | 12.2824(4) | 8.3320(3) |
| *b* (Å) | 29.8725(13) | 30.3634(11) | 14.0070(5) |
| *c* (Å) | 6.7654(3) | 6.8630(2) | 20.6378(7) |
| $\beta$ (°) | 96.925(5) | 100.444(2) | 90 |
| *V* (Å$^3$) | 2402.2(2) | 2517.05(14) | 2408.56(15) |
| Z | 4 | 4 | 4 |
| $\rho_{calc}$ (Mg/m$^3$) | 2.173 | 2.309 | 2.672 |
| $\mu$(K$\alpha$) (mm$^{-1}$) | 3.493 | 6.297 | 5.826 |
| No. reflns. | 18821 | 12583 | 26750 |
| θ Range (°) | 3.326–32.783 | 2.626–29.145 | 2.636–29.258 |
| Unique reflns. | 4175 | 3387 | 3384 |
| GOOF ($F^2$) | 1.064 | 1.147 | 1.152 |
| $R_{int}$ | 0.0498 | 0.0292 | 0.0505 |
| R1 [a] ($I \geq 2\sigma$) | 0.0359 | 0.0281 | 0.0360 |
| wR2 [b] ($I \geq 2\sigma$) | 0.0761 | 0.0586 | 0.0795 |

[a] $R1 = \Sigma||F_o| - |F_c||/\Sigma|F_o|$. [b] $wR2 = [\Sigma[w(F_o^2 - F_c^2)^2]/\Sigma[w(F_o^2)^2]]^{1/2}$. * Fw without solvent of crystallization.

## 3. Results and Discussion

### 3.1. Strength of the Halogen Bonds

The relative strength of halogen bonds can be estimated by the commonly used concept of the halogen bond interaction ratio, $R_{XB}$, (sometimes also called as normalized interaction distance). It is defined as $R_{XB} = d_{XB}/(X_{vdw} + B_{vdw})$, where $d_{XB}$ [Å] is the distance between the donor atom (X) and the acceptor atoms (B), divided by the sum of vdW radii [Å] of X and B, and the XB donor···acceptor (XB···A) [56–58]. Smaller values indicate stronger XB interactions. Small differences in $R_{XB}$ values do

not reflect differences in the overall structures. For example, structure 1 and 2 are isomorphous even if there is a small difference (2%) in the $R_{XB}$ values. Although the correlation between the crystal/overall structure and the XBs and their strength is not always straightforward, structural analysis provides a fast way to compare halogen bonds 116–125. The key structural parameters of the halogen bonds between the ruthenium coordinated halido ligand and the iodine of the DITFB XB donor in the three structures [Ru(bpy)$(CO)_2Cl_2$]·DITFB (**1**), [Ru(bpy)$(CO)_2Br_2$]·DITFB (2) and [Ru(bpy)$(CO)_2I_2$]·DITFB (3) are summarized in Table 2.

**Table 2.** Halogen bonds in 1–3 and in the [Ru(bpy)$(CO)_2X_2$]·$I_2$ XB complexes from Reference [31].

| **Compound** | **Ru-X···I (Å)** | **C-I···X (°)** | **M-X···I (°)** | **$R_{XB}$** |
|---|---|---|---|---|
| 1 | 3.1790(8) | 170.60(9) | 114.94(3) | 0.85 |
| 2 | 3.3191(4) | 171.34(10) | 112.108(14) | 0.87 |
| 3 | 3.5301(3) | 177.66(13) | 96.672(9) | 0.89 |
| **Ref. [31]** | Ru-X···I (Å) | I-I···X (°) | M-X···I (°) | $R_{XB}$ |
| Cl···$I_2$ | 3.0421(3) | 174.566(8) | 115.76(1) | 0.82 |
| Br···$I_2$ | 3.2938(4) | 170.28(1) | 101.3(1) | 0.86 |
| Br···$I_2$ | 3.3627(3) | 173.80(1) | 102.27(1) | 0.88 |
| Br···$I_2$ | 3.2381(3) | 175.405(9) | 101.66(1) | 0.85 |
| Br···$I_2$ | 3.3001(3) | 174.164(9) | 102.57(1) | 0.86 |
| I···$I_2$ | 3.1984(2) | 177.941(7) | 97.91(1) | 0.81 |
| I···$I_2$ | 3.7984(3) | 152.083(6) | 104.26(1) | 0.96 |
| I···$I_2$ | 3.2553(13) | 172.75(2) | 97.81(2) | 0.82 |
| I···$I_2$ | 3.4108(15) | 166.50(2) | 98.90(2) | 0.86 |

### *3.2. Crystal Structures*

Unlike in the case of $I_2$ XB donor reported earlier [31], the diiodotetrafluorobenze acts as a symmetrical XB donor bridging the Ru complexes in all three structures 1–3. In 1 and 2 the DITFB molecules are located on an inversion center, while in 3 it is located on a mirror plane. Similarly, the Ru atoms in 1 and 2 are located on a two-fold rotation axis, while in 3 the ruthenium atom is on a mirror plane. Due to the symmetry, the distances from both iodines of DITFB to the halido ligand of the metal complex are equal in all cases. This is due to the fact that when one end of the DITFB molecule forms a halogen bond, it does not change the behavior of the second iodine, which is possible in the case of $I_2$ linker [31].

The extended structures of Ru(bpy)$(CO)_2Cl_2$]·DITFB (1) and Ru(bpy)$(CO)_2Br_2$]·DITFB (2) are isomorphous zig-zag chains (Figure 2).

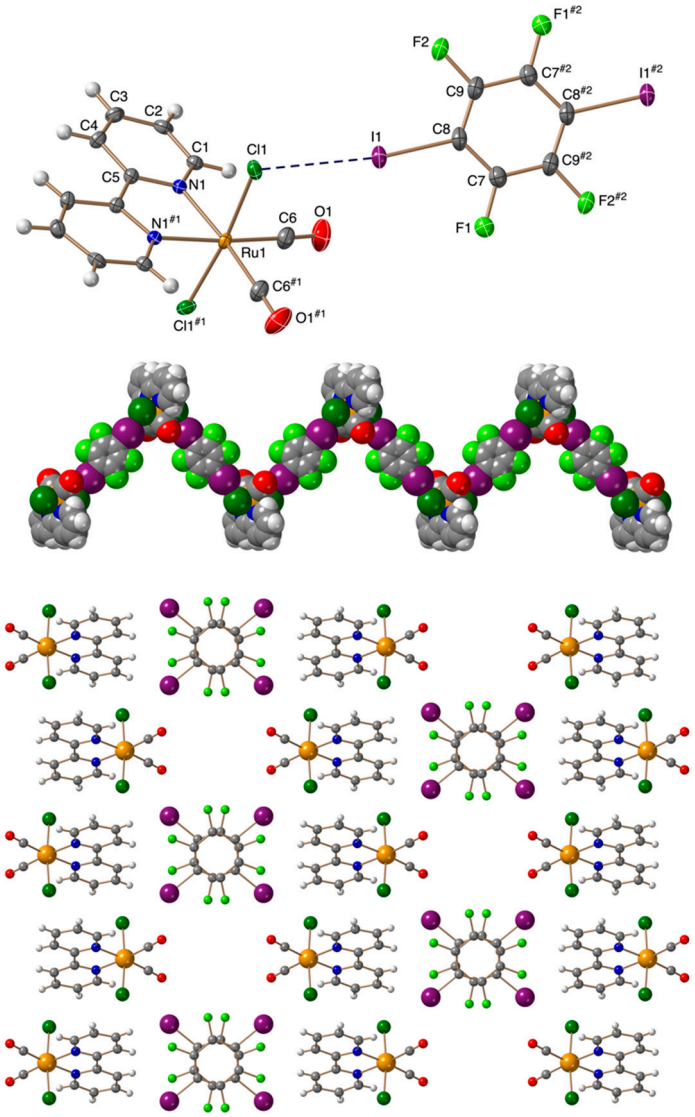


**Figure 2. Top**: TELP drawing of 1. Thermal ellipsoids have been drawn at 50% probability level. **Middle**: the polymeric zig-zag chain of 1. **Bottom**: Packing of 1 along the crystallographic c-axis. The corresponding figures of the isomorphous structure 2 are given in the Supplementary Materials. Symmetry transformations used to generate equivalent atoms: #1: −x + 1, y, −z + 3/2, #2: −x, −y + 1, −z + 1.

The TELP and packing images of 2 are given in the supplementeray material. In both 1 and 2 the halido ligands of the metal complexes are involved in halogen bonding and the halogen-halogen distances in both of these contacts are equal, as mentioned above. The M-Cl···I and M-Br···I contacts are 3.1790(8) Å and 3.3191(4) Å, respectively. The C-I···X angles are reasonably close to the linear contacts in both structures being 170.60(9)° for 1 and 171.34(10)° for 2. Both Ru-Cl···I and Ru-Br···I angles deviate quite clearly from the ideal 90° being 114.94(3)° and 112.108(14)° for 1 and 2, respectively. Such a deviation indicates that the electron density around the halido ligands is redistributed, increasing the electron density perpendicular to the Ru-X bond, but the effect is not particularly strong. In both 1 and 2, the aromatic DITFB donors are stacked with weak π–π interactions between the aromatic rings. The shortest carbon–carbon distances between the neighboring DITFB molecules range from 3.178(5) Å to 3.358(5) Å for 1 and from 3.165(5) Å to 3.685(5) Å for 2. In both 1 and 2 there are apparent voids in the structure (259 $Å^3$ and 310 $Å^3$, respectively). However, these voids are actually filled with disordered

solvent molecules, which were omitted from the crystal structure via SQUEEZE procedure (see X-Ray Structure Determination section).

The structure of 3 differs clearly from 1 and 2. Only one of the iodido ligands (I1) is involved in halogen bonding. The I1 of the Ru-complex acts as a ditopic XB acceptor linking simultaneously two DITFB donors (Figure 3).

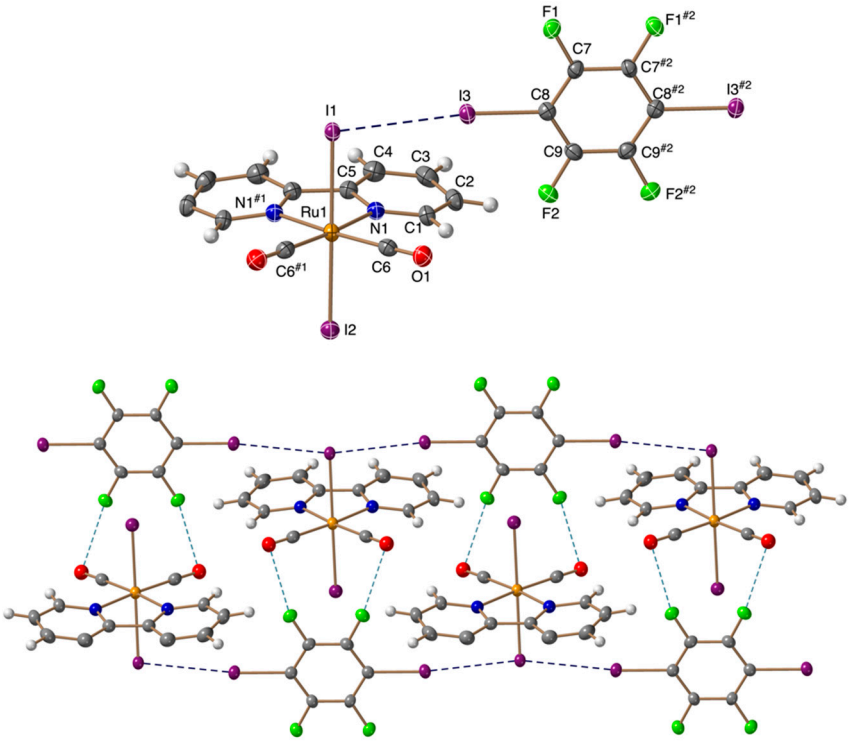


**Figure 3. Top**: TELP drawing of 3. **Bottom**: The chain of 3 with I···I halogen bonds and F···O contacts (2.833(5) Å). Symmetry transformations used to generate equivalent atoms: #1: x, −y + 1/2, z, #2: x, −y + 3/2, z.

The C-I···I angle of 177.66(13)° in 3 is closer to 180° and Ru-I···I angle of 96.672(9)° closer to 90° than the corresponding angles in 1 and 2. The Ru-I···I angle close to 90° is expected since the polarization of the iodido ligand is likely to be more efficient than the polarization of chlorido or bromido ligands. Just like in 1 and 2, all Ru-I···I halogen bond distances are also equal [3.5301(3) Å] in the structure 3. When the geometric parameters of 1–3 are compared to the values found in iodine linked $[Ru(bpy)(CO)_2X_2]\cdot I_2$ system some differences can be observed. First of all, based on the interaction ratios ($R_{XB}$) the order of the XB strength in 1–3 is increased systematically, i.e., X = Cl > Br > I (Table 2). In all cases, the $R_{XB}$ values were calculated by using Bondi van der Waals' radii [59]. Johnson et al. have reported the same order for the halogen-containing Pd pincer complexes with $I_2$ donors [14]. However, in $[Ru(bpy)(CO)_2X_2]\cdot I_2$ systems the order is less obvious. In these co-crystals the strength of the first halogen–halogen interaction between the halido ligand and $I_2$ have an impact on the XB donor strength of the second I atom [31]. The order of the strongest interactions in the $[Ru(bpy)(CO)_2X_2]\cdot I_2$ series is X = I > Cl > Br (see the Table 1). This is due to the increased electron sharing, i.e., covalency and charge transfer in the case of $[Ru(bpy)(CO)_2I_2]\cdot I_2$. In the case of Cl and Br complexes, the halogen bonds are more clearly electrostatic, and therefore the XB strength follows the same order as 2 and 3. In general, the $R_{XB}$ values found in structures 1–3 are slightly greater than the values found in other systems with halogen-containing ruthenium complexes and $I_2$ donors. Mosquera et al. have studied a series of $[Ru(CNR)_4X_2]\cdot I_2$ (X = Cl, Br, I) acceptors and their interactions with $I_2$ [45,47]. In these structures the M-X···I $R_{XB}$ value for X = Cl systems range between 0.78 and 0.85, for X = Br, $R_{XB}$ is 0.84 and for X = I the $R_{XB}$ value range between 0.79 and 0.84. Again, the order of the XB strength in these systems

is not so straightforward as in the case of 1–3. The $R_{XB}$ values in [Ru(dcbpy)$(CO)_2I_2$]·$I_2$ complexes are also somewhat smaller than in 3 with $R_{XB}$ = 0.79–0.82 [30] indicating again increased electron sharing and covalency between the XB donor and acceptor in $I_2$ donor systems. When structures 1–3 are compared with other, mainly electrostatic XB systems, such as trimethylplatinum(IV) iodide with iodopentafluoro-benzene XB donor, the observed $R_{XB}$ values match well [60]. This can also be seen if structures 1–3 are compared with the other metal complex adducts having DITFB as a halogen bond donor. The $R_{XB}$ values are nearly equal even if the metal and other ligands around the metal are different. For example, in PCPdX pincer complexes with DITFB donor the $R_{XB}$ values are 0.87 (X = Cl) and 0.88 (X = Br), respectively [14]. The slightly larger values found in these systems may be due to the steric hindrance reflected by the relatively wide M-X···I angle (131–143°). In the sterically more relaxed square planar cyclometallated [Pt(btpy)$(PPh_3)$Cl]·DITFB complex the $R_{XB}$ value for the Pt-Cl···I is 0.86, which is nearly the same value that can be found in structure 1 as well [29].

## 4. Conclusions

A series of [Ru(bpy)$(CO)_2X_2$]·DITFB (X = Cl, Br or I) halogen-bonded complexes were crystallized and analyzed. The [Ru(bpy)$(CO)_2Cl_2$]·DITFB and [Ru(bpy)$(CO)_2Br_2$]·DITFB complexes form isomorphous polymeric zig-zag chains where the 1,4-diiodotetrafluoro-benzenes (DITFB) act as symmetrical halogen bonding bridges linking metal complexes together. Although halogen bonds are relatively weak intermolecular interactions, they have a similar directional/directing role in crystallization as hydrogen bonds. Both halido ligands of the metal complex are involved in halogen bonding forming a single X···I contacts. The structure of [Ru(bpy)$(CO)_2I_2$]·DITFB differs from the other two systems. Only one of the iodido ligands is involved in XB interactions as a ditopic acceptor leading to a nearly linear polymeric chain of metal complexes. Furthermore, the neighboring chains are linked together via weak F···O contacts. The strength of the halogen bonds M-X···I, estimated by the halogen bond interaction ratio, $R_{XB}$, follows the order of nucleophilicity of the halido ligands being 0.85, 0.87, and 0.89 for X = Cl, X = Br, and X = I, respectively. When the [Ru(bpy)$(CO)_2X_2$]·DITFB series is compared with the corresponding series containing $I_2$ as the bridging halogen bond donors, the main differences arise from the behavior and nature of the XB donor. In the case of [Ru(bpy)$(CO)_2X_2$]·DITFB the halogen bonds, formed by the two iodines of DITFB, are equal in all structures. This differs from the behavior of the two ends of the $I_2$ linker, where the second contact depend on the strength and nature of the initial halogen bond. Almost solely electrostatically behaving DITFB provide thus a more predictably behaving linker for XB-bonded assemblies of metal halides.

**Supplementary Materials:** The following materials are available online at http://www.mdpi.com/2073-4352/9/6/319/s1, Figure S1: TELP drawing of structure 2; Figure S2: The polymeric zig-zag chains of 2; Figure S3: Packing of 2 along the crystallographic c-axis.

**Author Contributions:** Syntheses, initial X-ray structure characterization and original draft preparation X.D.; final structure analysis M.T.; manuscript review and editing: K.R.; conceptualization, supervision, funding acquisition and project administration, manuscript review and editing: M.H.

**Funding:** This research was funded by Academy of Finland, grant numbers 130571 and 295881.

**Conflicts of Interest:** The funders had no role in the design of the study; in the collection, analyses, or interpretation of data; in the writing of the manuscript, or in the decision to publish the results.

## References

1. Metrangolo, P.; Resnati, G.; Pilati, T.; Liantonio, R.; Meyer, F. Engineering functional materials by halogen bonding. *J. Polym. Sci. Part A Polym. Chem.* **2007**, *45*, 1–15. [CrossRef]
2. Cinčić, D.; Friščić, T.; Jones, W. Isostructural Materials Achieved by Using Structurally Equivalent Donors and Acceptors in Halogen-Bonded Cocrystals. *Chem. A Eur. J.* **2008**, *14*, 747–753. [CrossRef] [PubMed]
3. Nemec, V.; Fotović, L.; Friščić, T.; Cinčić, D. A large family of halogen-bonded cocrystals involving metal-organic building blocks with open coordination sites. *Cryst. Growth Des.* **2017**, *17*, 6169–6173. [CrossRef]

4. Ovens, J.S.; Geisheimer, A.R.; Bokov, A.A.; Ye, Z.G.; Leznoff, D.B. The Use of Polarizable $[AuX_2(CN)_2]^-$ (X = Br, I) Building Blocks Toward the Formation of Birefringent Coordination Polymers. *Inorg. Chem.* **2010**, *49*, 9609–9616. [CrossRef] [PubMed]
5. Rosokha, S.V.; Vinakos, M.K. Hybrid Network Formation via Halogen Bonding of the Neutral Bromo-Substituted Organic Molecules with Anionic Metal–Bromide Complexes. *Cryst. Growth Des.* **2012**, *12*, 4149–4156. [CrossRef]
6. Bertani, R.; Sgarbossa, P.; Venzo, A.; Lelj, F.; Amati, M.; Resnati, G.; Pilati, T.; Metrangolo, P.; Terraneo, G. Halogen bonding in metal-organic-supramolecular networks. *Coord. Chem. Rev.* **2010**, *254*, 677–695. [CrossRef]
7. Desiraju, G.R.; Ho, P.S.; Kloo, L.; Legon, A.C.; Marquardt, R.; Metrangolo, P.; Politzer, P.; Resnati, G.; Rissanen, K. Definition of the halogen bond (IUPAC Recommendations 2013). *Pure Appl. Chem.* **2013**, *85*, 1711–1713. [CrossRef]
8. Clark, T.; Hennemann, M.; Murray, J.S.; Politzer, P. Halogen bonding: The σ-hole. *J. Mol. Model.* **2007**, *13*, 291–296. [CrossRef] [PubMed]
9. Politzer, P.; Murray, J.S. σ-Holes and π-holes: Similarities and Differences. *J. Comput. Chem.* **2018**, *39*, 464–471. [CrossRef]
10. Politzer, P.; Murray, J.; Clark, T.; Resnati, G. The σ-Hole revisited. *Phys. Chem. Chem. Phys.* **2017**, *19*, 32166–32178. [CrossRef]
11. Esrafili, M.D.; Mousavian, P. The strengthening effect of a halogen, chalcogen or pnicogen bonding on halogen–π interaction: A comparative ab initio study. *Mol. Phys.* **2017**, *116*, 526–535. [CrossRef]
12. Cavallo, G.; Metrangolo, P.; Milani, R.; Pilati, T.; Priimagi, A.; Resnati, G.; Terraneo, G. The Halogen Bond. *Chem. Rev.* **2016**, *116*, 2478–2601. [CrossRef] [PubMed]
13. Cheng, N.; Liu, Y.; Zhang, C.; Liu, C. A theoretical study on the halogen bonding interactions of $C_6F_5I$ with a series of group 10 metal monohalides. *J. Mol. Model.* **2013**, *19*, 3821–3829. [CrossRef] [PubMed]
14. Johnson, M.T.; Džolić, Z.; Cetina, M.; Wendt, O.F.; Öhrström, L.; Rissanen, K. Neutral Organometallic Halogen Bond Acceptors: Halogen Bonding in Complexes of PCPPdX (X = Cl, Br, I) with Iodine ($I_2$), 1,4-Diiodotetrafluorobenzene (F4DIBz), and 1,4-Diiodooctafluorobutane (F8DIBu). *Cryst. Growth Des.* **2012**, *12*, 362–368. [CrossRef] [PubMed]
15. Tsuzuki, S.; Wakisaka, A.; Ono, T.; Sonoda, T. Magnitude and origin of the attraction and directionality of the halogen bonds of the complexes of $C_6F_5X$ and $C_6H_5X$ (X = I, Br, Cl and F) with pyridine. *Chem. Eur. J.* **2012**, *18*, 951–960. [CrossRef] [PubMed]
16. Politzer, P.; Murray, J.S.; Clark, T. Halogen bonding: An electrostatically-driven highly directional noncovalent interaction. *Phys. Chem. Chem. Phys.* **2010**, *12*, 7748–7757. [CrossRef] [PubMed]
17. Legon, A.C. The halogen bond: An interim perspective. *Phys. Chem. Chem. Phys.* **2010**, *12*, 7736–7747. [CrossRef]
18. Politzer, P.; Lane, P.; Concha, M.C.; Ma, Y.; Murray, J.S. An overview of halogen bonding. *J. Mol. Model.* **2007**, *13*, 305–311. [CrossRef]
19. Alkorta, I.; Sanchez-Sanz, G.; Elguero, J.; Del Bene, J.E. FCl:PCX complexes: Old and new types of halogen bonds. *J. Phys. Chem. A* **2012**, *116*, 2300–2308. [CrossRef]
20. Murray, J.S.; Macaveiu, L.; Politzer, P. Factors affecting the strengths of σ-hole electrostatic potentials. *J. Comput. Sci.* **2014**, *5*, 590–596. [CrossRef]
21. Zbačnik, M.; Pajski, M.; Stilinović, V.; Vitković, M.; Cinčić, D. The halogen bonding proclivity of the ortho-methoxy–hydroxy group in cocrystals of o-vanillin imines and diiodotetrafluoro-benzenes. *CrystEngComm* **2017**, *19*, 5576–5582.
22. Jeske, J.; du Mont, W.-W.; Jones, P.G. Iodophosphane Selenides: Building Blocks for Supramolecular Soft ± Soft. *Chem. Eur. J.* **1999**, *5*, 385–389. [CrossRef]
23. Madzhidov, T.I.; Chmutova, G.A.; Martín Pendás, Á. The nature of the interaction of organoselenium molecules with diiodine. *J. Phys. Chem. A* **2011**, *115*, 10069–10077. [CrossRef] [PubMed]
24. Politzer, P.; Murray, J.S. Halogen bonding and beyond: Factors influencing the nature of CN-R and SiN-R complexes with F-Cl and $Cl_2$. *Theor. Chem. Acc.* **2012**, *131*, 1–10. [CrossRef]
25. Ivanov, D.M.; Novikov, A.S.; Ananyev, I.V.; Kirina, Y.V.; Kukushkin, V.Y. Halogen bonding between metal centers and halocarbons. *Chem. Commun.* **2016**, *52*, 5565–5568. [CrossRef] [PubMed]

26. Groenewald, F.; Dillen, J.; Esterhuysen, C. Ligand-driven formation of halogen bonds involving Au(I) complexes. *New J. Chem.* **2018**, *42*, 10529–10538. [CrossRef]
27. Novikov, A.S. Theoretical confirmation of existence of X···Au non-covalent contacts. *Inorg. Chim. Acta* **2018**, *471*, 126–129. [CrossRef]
28. Brammer, L.; Mínguez Espallargas, G.; Libri, S. Combining metals with halogen bonds. *CrystEngComm* **2008**, *10*, 1712–1727. [CrossRef]
29. Sivchik, V.V.; Solomatina, A.I.; Chen, Y.T.; Karttunen, A.J.; Tunik, S.P.; Chou, P.T.; Koshevoy, I.O. Halogen Bonding to Amplify Luminescence: A Case Study Using a Platinum Cyclometalated Complex. *Angew. Chem. Int. Ed.* **2015**, *54*, 14057–14060. [CrossRef]
30. Tuikka, M.; Niskanen, M.; Hirva, P.; Rissanen, K.; Valkonen, A.; Haukka, M. Concerted halogen and hydrogen bonding in $[RuI_2(H_2dcbpy)(CO)_2]\cdots I_2\cdots(CH_3OH)\cdots I_2\cdots[RuI_2(H_2dcbpy)(CO)_2]$. *ChemComm* **2011**, *47*, 3427–3429. [CrossRef]
31. Ding, X.; Tuikka, M.J.; Hirva, P.; Kukushkin, V.Y.; Novikov, A.S.; Haukka, M. Fine-tuning halogen bonding properties of diiodine through halogen–halogen charge transfer—Extended $[Ru(2,2'\text{-bipyridine})(CO)_2X_2]\cdot I_2$ systems (X = Cl, Br, I). *CrystEngComm* **2016**, *18*, 1987–1995. [CrossRef]
32. Ding, X.; Tuikka, M.; Hirva, P.; Haukka, M. Halogen bond preferences of thiocyanate ligand coordinated to Ru(II)via sulphur atom. *Solid State Sci.* **2017**, *71*, 8–13. [CrossRef]
33. Lisac, K.; Cinčić, D. Simple design for metal-based halogen-bonded cocrystals utilizing the M–Cl···I motif. *CrystEngComm* **2018**, *20*, 5955–5963. [CrossRef]
34. Kia, R.; Mahmoudi, S.; Raithby, P.R. New rhenium-tricarbonyl complexes bearinghalogen-substituted bidentate ligands: Structural, computational and Hirshfeld surfaces studies. *CrystEngComm* **2019**, *21*, 77–93. [CrossRef]
35. Torubaev, Y.V.; Skabitskiy, I.V.; Rusina, P.; Pasynskii, A.A.; Raic, D.K.; Singhd, A. Organometallic halogen bond acceptors: Directionality, hybrid cocrystal precipitation, and blueshifted CO ligand vibrational band. *CrystEngComm* **2018**, *20*, 2258–2266. [CrossRef]
36. Scheiner, S. On the capability of metal–halogen groups to participate in halogen bonds. *CrystEngComm* **2019**, *21*, 2875–2883. [CrossRef]
37. Mills, A.M.; Van Beek, J.A.M.; Van Koten, G.; Spek, A.L. {2, 6-bis[(dimethylamino-κN)methyl]phenyl-κc}iodopalladium(ii) bis(diiodine). *Acta Cryst. Sect. C Cryst. Struct. Commun.* **2002**, *58*, m304–m306. [CrossRef]
38. Slugovc, C.; Kirchner, K.; Mereiter, K. (Hydridotripyrazolylborato)iodo{(1,2,5,6-η)-1-[(Z)-1-iodo-2-phenylethenyl]cycloocta-1,5-diene} ruthenium(II)–diiodine (2/1). *Acta Cryst. Sect. E Struct. Rep. Online* **2005**, *E61*, m1646–m1648. [CrossRef]
39. Palmer, S.M.; Stanton, J.L.; Jaggi, N.K.; Hoffman, B.M.; Ibers, J.A.; Schwartz, L.H. Preparation, Structures, and Physical Properties of Two Products from the Iodination of (Phthalocyaninato)iron(II). *Inorg. Chem.* **1985**, *24*, 2040–2046. [CrossRef]
40. Enders, M.; Ludwig, G.; Pritzkow, H. Nitrogen-functionalized cyclopentadienyl ligands with a rigid framework: Complexation behavior and properties of Cobalt(I), -(II), and -(III) half-sandwich complexes. *Organometallics* **2001**, *20*, 827–833. [CrossRef]
41. Zhao, S.-B.; Wang, R.-Y.; Wang, S. Reactivity of $SiMe_3$-and $SnR_3$-Functionalized Bis (7-azaindol-1-yl) methane with $[PtR_2(\mu\text{-}SMe_2)]_n$ (R)=Me, Ph) and the Resulting Pt(II) and Pt(IV) Complexes. *Organometallics* **2009**, *28*, 2572–2582. [CrossRef]
42. Buse, K.D.; Keller, H.J.; Pritzkow, H. Reaction of Molecular Iodine with cis-Dihalo (2,2′-bipyridyl) platinum(II) and cis-Dihalo (1,lQ-phenanthroline) platinum(II). Oxidative Addition and Inclusion Compounds. *Inorg. Chem.* **1977**, *16*, 1072–1076. [CrossRef]
43. Fanizzi, F.P.; Natile, G.; Lanfranchi, M.; Tiripicchio, A.; Laschi, F.; Zanello, P. Steric Crowding and Redox Reactivity in Platinum(II) and Platinum(IV) Complexes Containing Substituted 1,10-Phenanthrolines. *Inorg. Chem.* **1996**, *35*, 3173–3182. [CrossRef]
44. Safa, M.; Puddephatt, R.J. Organoplatinum complexes with an ester substituted bipyridine ligand: Oxidative addition and supramolecular chemistry. *J. Organomet. Chem.* **2013**, *724*, 7–16. [CrossRef]
45. Mosquera, M.E.G.; Egido, I.; Hortelano, C.; López-López, M.; Gómez-Sal, P. Comparison of Halogen Bonding networks with Ru(II) complexes and analysis of the influence of the XB interaction on their reactivity. *Faraday Discuss.* **2017**, *203*, 257–283. [CrossRef]

46. Hewison, L.; Crook, S.H.; Mann, B.E.; Meijer, A.J.H.M.; Adams, H.; Sawle, P.; Motterlini, R.A. New types of CO-releasing molecules (CO-RMs), based on iron dithiocarbamate complexes and $[Fe(CO)_3I(S_2COEt)]$. *Organometallics* **2012**, *31*, 5823–5834. [CrossRef]
47. Mosquera, M.E.G.; Gomez-Sal, P.; Diaz, I.; Aguirre, L.M.; Ienco, A.; Manca, G.; Mealli, C. Intriguing $I_2$ Reduction in the Iodide for Chloride Ligand Substitution at a Ru(II) Complex: Role of Mixed Trihalides in the Redox Mechanism. *Inorg. Chem.* **2016**, *55*, 283–291. [CrossRef] [PubMed]
48. Coronado, E.; Day, P. Magnetic Molecular Conductors. *Chem. Rev.* **2004**, *104*, 5419–5448. [CrossRef] [PubMed]
49. Haukka, M.; Kiviaho, J.; Ahlgrén, M.; Pakkanen, T.A. Studies on Catalytically Active Ruthenium Carbonyl Bipyridine Systems. Synthesis and Structural Characterization of $[Ru(bpy)(CO)_2Cl_2]$, $[Ru(bpy)(CO)_2Cl(C(O)OCH_3)]$, $[Ru(bpy)(CO)_2Cl]_2$, and $[Ru(bpy)(CO)_2ClH]$ (bpy = 2,2′-Bipyridine). *Organometallics* **1995**, *14*, 825–833. [CrossRef]
50. Haukka, M.; Ahlgrén, M.; Pakkanen, T.A. Reactions of $[Ru(bipy)(CO)_2Cl_2]$ in aqueous HX and HX–$HNO_3$ solutions (X = F, Br or I; bipy = 2,2′-bipyridine). *J. Chem. Soc. Dalton Trans.* **1996**, 1927–1933. [CrossRef]
51. Rikagu Oxford Diffraction. *CrysAlisPro V. 1.171.37.35*; Rikagu Oxford Diffraction: Yarnton, Oxfordshire, UK, 2015.
52. Bruker AXS. *APEX2-Software Suite for Crystallographic Programs*; Bruker AXS, Inc.: Madison, WI, USA, 2009.
53. Palatinus, L.; Chapuis, G. Superflip—A computer program for the solution of crystal structures by charge flipping in arbitrary dimensions. *J. Appl. Cryst.* **2007**, *40*, 786–790. [CrossRef]
54. Sheldrick, G.M. Crystal structure refinement with *SHELXL*. *Acta Cryst.* **2015**, *C71*, 3–8.
55. Spek, A.L. Structure validation in chemical crystallography. *Acta Cryst.* **2009**, *D65*, 148–155. [CrossRef] [PubMed]
56. Lommerse, P.M.; Stone, A.J.; Taylor, R.; Allen, F.H. The nature and geometry of intermolecular interactions between halogens and oxygen or nitrogen. *J. Am. Chem. Soc.* **1996**, *118*, 3108–3116. [CrossRef]
57. Brammer, L.; Bruton, E.A.; Sherwood, P. Understanding the Behavior of Halogens as Hydrogen Bond Acceptors. *Cryst. Growth Des.* **2001**, *1*, 277–290. [CrossRef]
58. Zordan, F.; Brammer, L.; Sherwood, P. Supramolecular Chemistry of Halogens: Complementary Features of Inorganic (M−X) and Organic (C−X′) Halogens Applied to M−X···X′−C Halogen Bond Formation. *J. Am. Chem. Soc.* **2005**, *127*, 5979–5989. [CrossRef] [PubMed]
59. Bondi, A. van der Waals Volumes and Radii. *J. Phys. Chem.* **1964**, *68*, 441–451. [CrossRef]
60. Ghosh, B.N.; Lahtinen, M.; Kalenius, E.; Mal, P.; Rissanen, K. 2,2′:6′,2″-Terpyridine trimethylplatinum(IV) iodide complexes as bifunctional halogen bond acceptors. *Cryst. Growth Des.* **2016**, *16*, 2527–2534. [CrossRef]